Discovery of an ergosterol-signaling factor that regulates *Trypanosoma brucei* growth[s]

Brad A. Haubrich,[1,2,]* Ujjal K. Singha,[1,†] Matthew B. Miller,* Craigen R. Nes,[3,]*
Hosanna Anyatonwu,* Laurence Lecordier,[§] Presheet Patkar,* David J. Leaver,*,**
Fernando Villalta,[†] Benoit Vanhollebeke,[§] Minu Chaudhuri,[†] and W. David Nes[4,]*

Center for Chemical Biology and Department of Chemistry and Biochemistry,* Texas Tech University, Lubbock, TX 79409; Department of Microbiology and Immunology,[†] Meharry Medical College, Nashville, TN 37208; Laboratoire de Parasitologie Moléculaire,[§] IBMM, Université Libre de Bruxelles, B6041 Gosselies, Belgium; and Institute of Chemistry and Biomedical Sciences,** Nanjing University, Nanjing 210023, People's Republic of China

Abstract Ergosterol biosynthesis and homeostasis in the parasitic protozoan *Trypanosoma brucei* was analyzed by RNAi silencing and inhibition of sterol C24β-methyltransferase (*Tb*SMT) and sterol 14α-demethylase [*Tb*SDM (*Tb*CYP51)] to explore the functions of sterols in *T. brucei* growth. Inhibition of the amount or activity of these enzymes depletes ergosterol from cells at <6 fg/cell for procyclic form (PCF) cells or <0.01 fg/cell for bloodstream form (BSF) cells and reduces infectivity in a mouse model of infection. Silencing of *Tb*SMT expression by RNAi in PCF or BSF in combination with 25-azalanosterol (AZA) inhibited parasite growth and this inhibition was restored completely by adding synergistic cholesterol (7.8 μM from lipid-depleted media) with small amounts of ergosterol (1.2 μM) to the medium. These observations are consistent with the proposed requirement for ergosterol as a signaling factor to spark cell proliferation while imported cholesterol or the endogenously formed cholesta-5,7,24-trienol act as bulk membrane components. To test the potential chemotherapeutic importance of disrupting ergosterol biosynthesis using pairs of mechanism-based inhibitors that block two enzymes in the post-squalene segment, parasites were treated with AZA and itraconazole at 1 μM each (ED$_{50}$ values) resulting in parasite death.▮▮ Taken together, our results demonstrate that the ergosterol pathway is a prime drug target for intervention in *T. brucei* infection.—Haubrich, B. A., U. K. Singha, M. B. Miller, C. R. Nes, H. Anyatonwu, L. Lecordier, P. Patkar, D. J. Leaver, F. Villalta, B. Vanhollebeke, M. Chaudhuri, and W. D. Nes. **Discovery of an ergosterol-signaling factor that regulates *Trypanosoma brucei* growth.** *J. Lipid Res.* 2015. 56: 331–341.

Supplementary key words ergosterol biosynthesis • cholesterol • sparking function • inhibitor • ribonucleic acid interference • knockdown • anti-parasite drugs

Trypanosomes carried by the tsetse fly are responsible for African sleeping sickness, a serious health risk in Sub-Saharan Africa which is spreading in travelers to Europe and the United States (1–3). Sterol biosynthesis is an extremely important area of biochemical difference between these protozoan parasites and their animal hosts that might be exploited in the development of new chemotherapeutic leads. Therefore, it is notable that *Trypanosoma brucei* operates a phyla-specific ergosterol biosynthesis pathway distinct from other Kinetoplastids or fungi, and produce a sterol metabolome that is different from animals (**Fig. 1**) (4–6). The uniqueness of ergosterol biosynthesis and homeostasis in *T. brucei* resides primarily in formation of a 24β-methyl group in the sterol side chain structure catalyzed by sterol C24-methyl transferase (*Tb*SMT) and in the amount of final product, ergosterol, utilized in growth support. Detailed studies of metabolism using ^{13}C- and ^{2}H-labeled intermediates supported by mechanistic analysis of the cloned *Tb*SMT reveal that the introduction of the C24β-methyl group in the sterol side chain proceeds in *T. brucei* by a methylation-deprotonation $\Delta^{25(27)}$-olefin
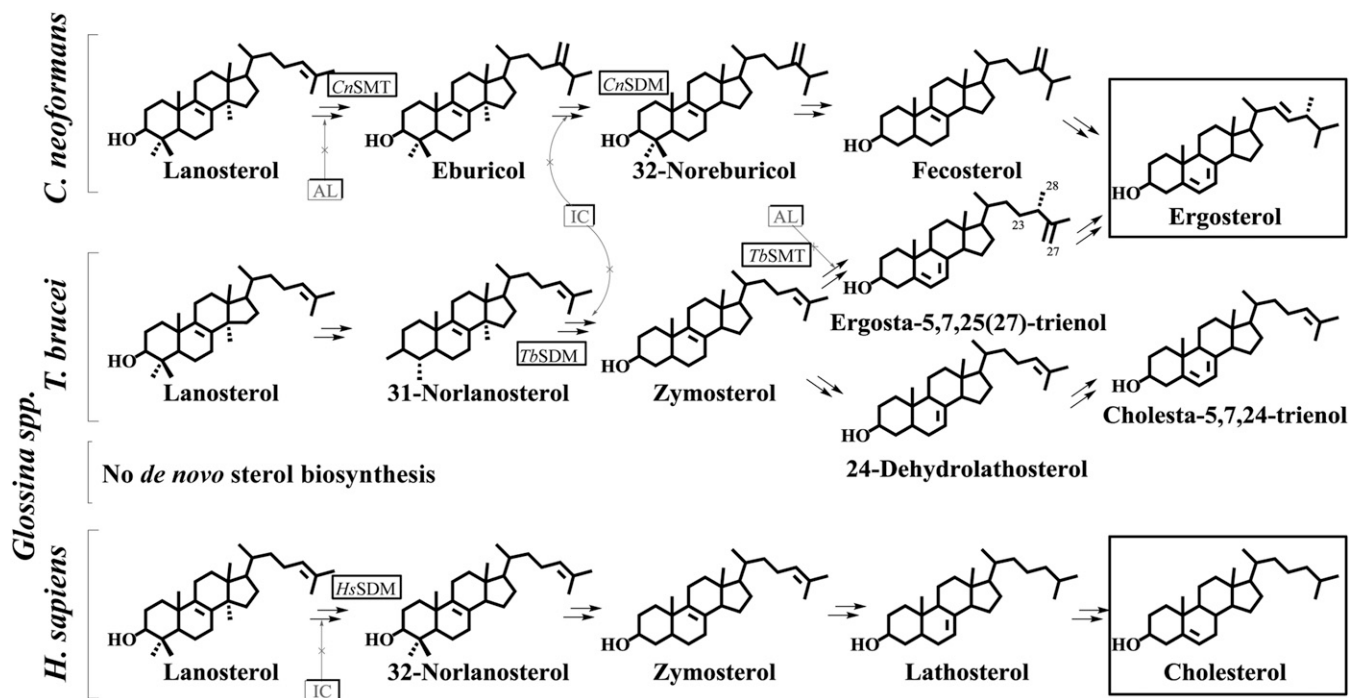
Fig. 1. Comparative sterol biosynthesis pathways across kingdoms showing representative routes to fungal ergosterol (*Cryptococcus neoformans* associated with AIDS) and protozoan (*T. brucei* associated with sleeping sickness) and animal cholesterol (*Homo sapiens* as the human host). Insects do not synthesize sterols as typified by the vector of *T. brucei* Glossina spp. [adapted from (5–7, 46. Boxed structures represent final products of functional significance.

pathway, which likely diverged from the methylation-deprotonation $\Delta^{24(28)}$-olefin pathway yielding fungal ergosterol very early in the evolution of eukaryotes (6–8).

T. brucei encounters diverse environments during its life cycle, with the different stages taking on very different sterol compositions. Despite having an intact ergosterol biosynthesis pathway in the procyclic forms (PCFs), the bloodstream forms (BSFs) are generally considered to lack ergosterol biosynthesis and to be auxotrophic for sterol (9–13). At this stage, cells satisfy their sterol requirements through dietary supplementation of cholesterol via lipoproteins in full-growth medium (FGM) present in the blood meal (10, 11). Consequently, the existence of a sterol uptake process which permits the formation of BSF membranes containing exclusively cholesterol could provide resistance to a range of antifungal drugs, e.g., amphotericin B, that function typically in membranes formed by ergosterol (14, 15). However, all the genes for ergosterol biosynthesis have been found recently to be expressed in BSF (16, 17) and inhibitors of the post-squalene portion of ergosterol biosynthesis can inhibit growth of BSFs (4, 18–20); therefore, the ability for BSFs to grow as an ergosterol-depleted protozoan with dietary cholesterol as an ergosterol surrogate remains enigmatic.

In nature, sterols are chiefly used as structural components of membranes (21, 22). Mammalian cell membranes are considered to be more flexible than fungal or protozoan cell membranes (23), and the chemodiversity in sterol biosynthesis may contribute to their architectural suitability (24). However, there is growing evidence that the sterol requirements for membrane structures across

kingdoms are rather broad and can be met by several closely related compounds. Thus, cholesterol can be shown to replace ergosterol in yeast membranes and phytosterols can be shown to replace cholesterol in animal membranes (25–28). On the other hand, functional diversity of sterols is reported to exist, with emphasis on the variation in sterol side chain structures which contribute to the regulatory role that sterols per se may play, apart from modulating the bulk physical properties of the membrane. For yeast, the "regulatory role" of ergosterol, also referred to as sparking (29), is to provide direct integration of a chemical switch into membrane domains to signal cell proliferation and possibly affect cell shape (29–31). The phenomenon by which ergosterol can play dual roles in yeast has been defined as sterol synergism (26) and the two kinds of function, bulk and sparking, can be distinguished quantitatively from each other by differing sensitivities to the 24β-methyl group of the sterol's structure (31).

Given the possibility that BSFs generate ergosterol in small amounts to promote growth and accessibility of very few therapeutic drugs, with many produced over 30 years ago, and toxicity issues (32, 33), we examined the concentration dependence of ergosterol in *T. brucei* growth and evaluated the potential use of targeted enzymes of ergosterol biosynthesis for future therapies. Here we demonstrate that quantitative differences in the ergosterol content of PCFs or BSFs of different infective types contribute to variations in the growth response. Additionally, by examination of the knockdown of *Tb*SMT and *Tb*SDM (sterol 14α-demethylase) gene expression together with inhibitor

treatment of PCFs and BSFs cultured in vitro or in vivo using infected mice, we show that C24-sterol methylation and ergosterol are the sine qua non of sparking trypanosome proliferation.

EXPERIMENTAL PROCEDURES

Instrumental methods

Sterol compounds, referenced to the retention time of cholesterol in capillary GC at 13.8 min, or somewhat longer depending on whether the column length was clipped due to age, and HPLC at 17 or 22 min, depending on the particle size of the stationary phase of 3 and 5 μm, respectively, were quantified by integration of the detector signal (flame ionization detector in GC and UV at 210 nm in HPLC, from 10 to 30 min). Products were routinely identified by their retention times in GC and electron-impact spectrum with those of reference samples. For the identification of select products, preparative HPLC was carried out on large amounts of cell pellet using a Phenomenex analytical Luna C_{18}-column 5 μm particle size (eluted with methanol at 20°C at 1 ml/min) linked to a diode array detector which provided UV spectra at 210 and 282 nm; fractionation was followed by GC-MS (ZB-5 capillary column of 30 m) using a Hewlet-Packard LS 6500 gas chromatograph interfaced to a Hewlet-Packard 5973 mass spectrometer.

Materials

Cholesterol and ergosterol were recrystallized from commercial samples and lanosterol was purified by HPLC from a mixture of compounds in the commercial lanosterol sample purchased from Sigma (1). The [methyl-$^3H_3$]AdoMet (10–15 Ci-mmol), which was diluted to 10 μCi/μmol for the activity assays, was purchased from Perkin Elmer. Itraconazole (ITC) was purchased from Sigma. The 25-azalanosterol (AZA) and 25-thialanosterol sulfonium salts were prepared as previously reported (34, 35).

Cell cultures and growth studies

T. brucei strains 427 and 328 PCF cells were grown in SDM-79 medium supplemented with 10% heat-inactivated FBS (Atlanta Biologicals), referred to as the FGM at 27°C. The *T. brucei* 427 (29-13) cell line, resistant to hygromycin (Invitrogen) and neomycin (G418) (Invitrogen), expressing the tetracycline repressor (TetR) gene and T7RNA polymerase, were grown in the same medium containing appropriate antibiotics (hygromycin, 50 μg/ml; G418, 15 μg/ml) (36, 37). BSF cells were maintained in HMI-9 medium supplemented with 10% heat-inactivated FBS (Atlanta Biologicals) and 10% Serum Plus (SAFC Biosciences), which is a FGM. The *T. brucei* 427 single marker cell line, resistant to G418 and expressing the TetR gene and T7RNA polymerase, was grown in the same medium containing G418 (2.5 μg/ml). For preparation of lipid-depleted medium (LDM), PCFs in SDM-79 medium were supplemented with 10% heat-inactivated lipid-free FBS (Sigma-Aldrich). For a low-cholesterol medium, the BSF cells were grown in HMI-9 medium containing 10% lipid-free heat-inactivated FBS (Sigma-Aldrich). For growth curves, SMT and SDM RNAi engineered cells were diluted into FGM or LDM, induced by RNAi by the addition of doxycycline (DOX) (1 μg/ml final), and cell density monitored for another 4–6 days. Typically, procyclic cells were inoculated at $2–3 \times 10^6$ cells/ml and BSF cells inoculated at 1×10^5 cells/ml in medium containing antibiotic and cultured for 6–8 days. Cell densities were maintained in the range of $0.5–1 \times 10^7$ cells/ml for the PCF and $0.1–1 \times 10^6$ cells/ml

for the BSF by reinoculation in fresh medium. Cells were harvested by centrifugation. *Tb*SMT inhibitors and ITC were added to PCF or BSF cells from stock solutions in dimethyl sulphoxide, such that the organic solvent was less than 1% (v/v) of total culture volume. Five different concentrations of each compound were tested in triplicate between 0 (control) and 10 μM; the 50% growth inhibition reported as the IC_{50} relative to the growth of control. Cell densities were determined using a Neubauer hemocytometer counter. The cumulative cell number was plotted versus time of growth.

Human epithelial cells (HEK 293T) were purchased from ATCC (Manassas, VA). HEK cells were cultured at 37°C in a humidified 5% CO_2 incubator in DMEM (Invitrogen, Carlsbad, CA) supplemented with 10% FBS. Cell viability was checked by trypan blue dye exclusion as described (38, 39). A set of subspecies of *T. brucei* trypomastigotes, *T. brucei brucei* (strains 328-114 and 427), *T. brucei rhodesiense* (Etatl.2S), and *T. brucei gambiense* (LiTatl.3), were cultured as described above (40).

Northern blot analysis

Total RNA was isolated from *T. brucei* PCF and BSF SMT RNAi and SDM RNAi cell lines grown in the presence and absence of DOX using Trizol reagent (Invitrogen) and Northern blot analysis was performed as described (41). Total RNA (5–10 μg) was loaded per lane and the blot was probed with ^{32}P-labeled DNA probe corresponding to the same SMT sequence corresponding to the SMT RNAi.

Inhibition of *Tb*SMT activity

Initially, the steady-state kinetic parameters, K_m and V_{max}, were established using lysate of *Escherichia coli* (8). Zymosterol concentration was varied from 5 to 150 μM and [$^3H_3$-methyl]S-adenosyl-L-methionine (SAM) concentration was fixed at 100 μM and the assay was performed under initial velocity conditions on soluble protein. The resulting kinetics for zymosterol conversion to ergosta-8,25(27)-dienol were calculated by fitting the liquid scintillation data to the Michaelis-Menten equation using the Enzyme Kinetic Module from SigmaPlot (42). The K_m and V_{max} values generated for zymosterol against cloned *Tb*SMT for experiments performed herein were essentially the same as those reported in (8). Inhibitor dissociation constants of 25-thialanosterol sulfonium salt and lanosterol for *Tb*SMT were based on steady-state experiments for assays performed in triplicate at varied zymosterol concentrations from 5 to 100 μM and [$^3H_3$-methyl]SAM fixed at 100 mM in the presence of inhibitor varied in the amount from 5 to 75 nM (25-thialanosterol sulflonium salt) or from 10 to 150 μM (lanosterol), while the data for AZA was previously reported in (8). Minimal variation was detected in the experimentally determined kinetic constants with standard errors of 2–10% between trials.

Sterol isolation and analysis

T. brucei cell pellets were saponified directly in 10% KOH in 80% aqueous methanol at the reflux temperature for 1 h, which yielded total sterol (free plus esterified sterols). The neutral lipids obtained by dilution with water and extraction with hexane (Fisher) after the saponification were analyzed by GC (3% SE-30 pack column operated isothermally at 245°C). Total sterols in the nonsaponifiable lipid fraction were purified on an Agilent 1100 series HPLC system coupled to a diode array detector. The total sterols were loaded onto a C_{18} reversed phase analytical column (Phenomenex, 4 μm) eluted isocratically with methanol at a flow rate of 1 ml/min. The standard for HPLC data was cholesterol, and the rates of movement are given relative to cholesterol (α_c). HPLC fractions in the sterol region of the chromatogram (α_c 0.5–2.0)

were collected and analyzed by GC-MS with a Hewlett-Packard LS 6500 gas chromatograph at 70 eV. GC was performed using an Agilent ZB-5 column (30 m × 25 µm in diameter). Cholesterol was the standard for determination of the relative retention time (RRT_c). Quantitation of the amounts of unlabeled sterols was accomplished by GC with a standard curve for cholesterol. To several cell pellets undergoing the saponification process, a known amount of 5α-cholestane was added as an internal standard.

Generation of *T. brucei* RNAi cell lines

To prepare the construct for *TbSMT* double stranded RNA expression, the 588 bp fragment of the coding region was PCR amplified from *T. brucei* genomic DNA by using high-fidelity pfu polymerase (Stratagen). Sense and antisense primers containing the restriction sites for BamH1 and HindIII at the 5′ ends were *TbSMT* For 5′agtcggatcctgtgaatggcgatgtgaatgc3′ and *TbSMT*Rev 5′agtcaagcttcatacaggtccgtcaaacaccac3′, respectively. The amplified product was cloned into the BamH1/HindIII sites of a tetracycline-inducible dual-promoter plasmid vector, p2T7^{Ti}-177 (43). The construct for *TbSMT* RNAi was verified by sequencing. The purified plasmid DNA was linearized by NotI and transfected into *T. brucei* 427 29-13 PCF and the single marker 427 BSF cells expressing T7 polymerase and TetR proteins according to standard protocol (37). Transfectants were selected by phleomycin (2.5 µg/ml). Similar approaches were used to generate the *Tb*SDM RNAi cell line.

Mouse infection

Sixteen male Balb/C mice (10–12 weeks old) were divided into two groups of eight mice in each group. Mice were pretreated for 5 days and continued throughout the experiment with either DOX (50 mg/kg body weight/day) in 5% sucrose water (*SMT* RNAi group) or 5% sucrose water alone (control group) via oral gavages. DOX is the water soluble and bio-available form of tetracycline, which induces the expression of RNAi in vivo but does not itself affect the infection process. Each mouse was then infected with 1×10^4 *T. brucei* BSF *SMT* RNAi cells by intraperitoneal injection. Parasitemia was measured each day in tail-vein blood from mice until the parasite count reached within the range of $4–8 \times 10^8$/ml. At this point mice were euthanized according to the Institutional Animal Care guidelines. Mice were also monitored daily for general appearance, behavior, and weight loss. If a mouse showed obvious distress and >20% weight loss, the mouse was euthanized. The protocols involving mice were approved by the Institutional Care and Use Committee of the Meharry Medical College.

Treatment of SMT inhibitors on *T. brucei* BSF in vivo

There were three groups of mice and each group had six mice: group I, control, treated with vesicle; group II, treated with aza-lano; and group III, treated with thia-lano. Mice were infected with BSF (10^4 parasites/mouse) by ip injection. Inhibitors were adminstered (50 mg/kg each, ip) after 2 h of injection of parasites and on each day post infection. The parasitemia level was monitored by counting cell numbers (bloodstream trypanosomes) in blood each day after infection. Mice were euthanized when the blood parasitemia level reached $4–8 \times 10^8$/ml.

RESULTS

Ergosterol is synthesized variably in wild-type PCF and BSF

Growth of wild-type PCF strain 427 in FGM, which provides 678 µM (262 µg/ml) cholesterol (4), followed a logarithmic course with a doubling time of 12 h and yielded cell densities at 6 days of $1–3 \times 10^7$ per ml. When these cells were extracted, the GC-MS analysis of the neutral lipid fraction showed the presence of cholesterol and a set of endogenously formed 24-desalkyl (mostly cholesta-5,7,24-trienol) and 24-alkyl sterols (mostly ergosta-5,7,25(27)-trienol) in approximate 50:50 ratio (**Table 1**). Ergosterol in GC at RRT_c 1.11 was determined to be in trace amounts. However, this compound was barely detectable by GC-MS analysis (supplementary Figs. 1–5, supplementary Table 1) because it chromatographs underneath the cholesta-5,7,24-trienol peak at RRT_c 1.10, which dominates the neutral lipid fraction. Ergosterol in the neutral lipid fraction could be quantified accurately by HPLC-UV scanning at 282 nm, which is the λ_{max} for the absorption band of the $\Delta^{5,7}$-diene system. Using a combination of GC-MS and HPLC-UV scanning, the amount of total sterol in the cells was estimated to be 163 fg/cell (±10 fg/cell) and the amount of ergosterol was approximately 6 fg/cell (±1 fg/cell) or 3.5% of the total sterol; co-metabolite analysis and determination of the ergosterol content of *T. brucei* strain 328 indicated these cells produce a similar sterol profile to strain 427.

A different situation was obtained when the serum lipoproteins were removed from the media, i.e., LDM, which provides approximately 7.8 µM (3 µg/ml) cholesterol [(4) reports the amount of cholesterol in lipid depleted medium and we converted that amount to µM.]. In this case, the total sterol was approximately the same as for cells cultured in FGM at 145 fg/cell (±10 fg/cell), while the cellular cholesterol was minor (21% total sterol); the sterol mixture was mostly cholesta-5,7,24-trienol and ergosta-5,7,25(27)-trienol (supplementary Table 1) and cells grew to a lower density at 6 days of $4–5 \times 10^6$ cells per ml. Coincidently, the amount of cellular ergosterol was drastically reduced to a level of approximately 0.9 fg/cell (±0.1 fg/cell) or 0.6% total sterol.

Subsequent experiments showed, however, that the concentration of ergosterol in BSF could be even much lower than in the PCF, making routine GC-MS analysis problematic for quantification of this compound. To generate a more exacting analysis, we repeated our previous efforts at sterol analysis of cultured cells by harvesting much larger cell pellets of the previously studied *T. brucei brucei* strain 427. In addition, we cultured large amounts of strain *T. brucei brucei* 328 and two related subspecies, *T. brucei rhodesiense* and *T. brucei gambiense*, of cell numbers that ranged from 3×10^9 to 7×10^{10}. When strain *T. brucei brucei* 427 was extracted, GC-MS analysis of the neutral lipids showed a mixture of cholesterol and a set of phytosterols of dietary origin, which eluted from 16 to 18 min (**Fig. 2A**), in agreement with previous studies (4). The sterol profile of strain 427 was similar to that of the other strains and subspecies examined with the amount of total sterol estimated to be 150 fg/cell (±10 fg/cell).

The neutral lipid fractions of *T. brucei brucei* (strains 427 and 328), *T. brucei gambiense,* and *T. brucei rhodesiense* were chromatographed by HPLC. The total sterols in the combined fractions (α_c 0.5–0.95) from semi-preparative

TABLE 1. Sensitivities and sterol composition of *T. brucei* cells to silencing *Tb*SMT or *Tb*SDM and ergosterol biosynthesis inhibitors

Treatment	PCF[a] (µM)	BSF[a] (µM)	HEK[a] (µM)	TI[b]	Sterol Composition (% Total)[c]			
					Cholesterol	24-Desalkyl Sterols	24-Alkyl Sterols	Erg[d]
Control	ND	ND	ND	ND	51	40	9	3.5
RNAi *Tb*SMT	ND	ND	ND	ND	76	24	Trace	0.3
RNAi *Tb*SDM	ND	ND	ND	ND	83	12	5	0.3
AZA	1	2	>50	25	90	10	Trace	NP
25-Thialanosterol sulfonium salt	2	2	>50	25	92	7	Trace	NP
ITC	3	3	>100	33	87	4	9	NP

TI, therapeutic index; Erg, ergosterol; ND, not determined; NP, not present within routine limits of detection by GC-MS analysis.

[a]The values were calculated from the dose-response curves of cultures in FGM. The dose causing a 50% cell growth inhibition, ED_{50} <10 µM being proposed as a threshold to consider a compound as a potential antisleeping sickness drug (45).

[b]Therapeutic index ED_{50} HEK/ED_{50} BSF. Each value is a mean of three independent experiments which varied by 0.2–0.3 µM.

[c]Sterol composition of DOX-induced RNAi cell lines and treated cells at ED_{90} drug concentration; trace is <1% total sterol.

[d]Ergosterol content in the total sterols.

HPLC (Luna C18 column) were injected in 100 µl aliquots into an analytical HPLC (Prodigy column) affording trace amounts of ergosterol. HPLC-UV scanning showed ergosterol was present in all the cells (Fig. 2B). The identity of the recovered material was confirmed by GC-MS analysis as ergosterol (RRT$_c$ 1.10; M$^+$ at m/z 396, which agreed with an authentic specimen). HPLC-UV scanning of the ergosterol in BSF cultured in FGM showed 0.01 fg/cell (±0.01 fg/cell), and in cells cultured in LDM showed five to ten times less ergosterol at 0.005–0.001 fg/cell (±0.01 fg/cell).
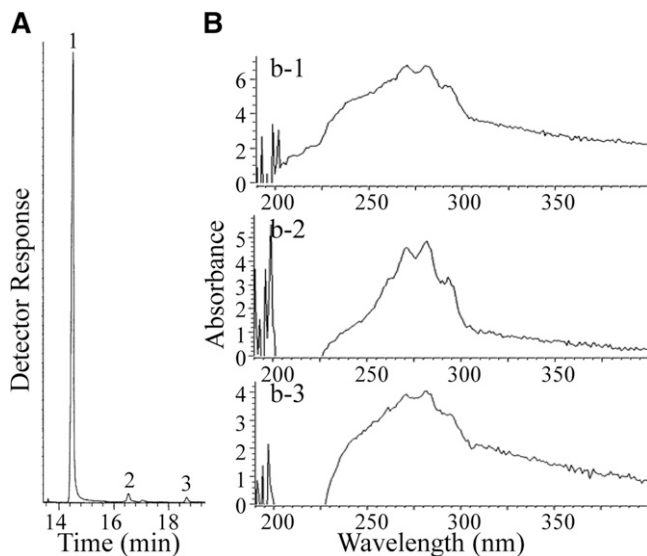

Fig. 2. Sterol analysis of BSFs of different origins. A: Representative total ion current chromatogram of neutral lipids from *T. brucei* BSFs [peak 1, cholesterol; peak 2, campesterol; peak 3, sitosterol cf. (4)]. B: UV spectra of HPLC fraction which had the α_c of ergosterol derived by semi-preparative HPLC and analytical HPLC of the neutral lipid fraction of *T. brucei brucei* (b-1), *T. brucei gambiense* (b-2), and *T. brucei rhodesiense* (b-3), as described in text.

Ablation of *Tb*SMT and *Tb*SDM gene expression and inhibitor treatment decreases ergosterol production in PCF

To assess the importance of ergosterol biosynthesis enzymes for the parasite's metabolism, we first down-regulated *Tb*SMT and *Tb*SDM gene expression by RNA silencing in PCF. In the absence of DOX, the resulting RNAi cell lines grew in a manner similar to the wild-type trypanosome cell line, with cell densities at day 7 yielding 8×10^6 cells/ml or $1–3 \times 10^6$ cells/ml in FGM and LDM, respectively (**Fig. 3A, B**). However, in the presence of DOX, growth was significantly reduced with cell densities at day 7 yielding $2–3 \times 10^6$/ml or below in FGM and LDM, respectively, or in LDM, *Tb*SDM RNAi plus DOX lines did not grow at all. Northern blot analysis showed that *Tb*SMT and *Tb*SDM transcript levels were undetectable within 1–2 days of DOX pressure (Fig. 3C, D), proving silencing of the genes of ergosterol biosynthesis, as expected. The effect of the RNAi on cell growth was more pronounced on later days because of the gradual loss of these gene products by cell division and product turnover. The amount of total sterol, 161 fg/cell (±10 fg/cell), in engineered cells in FGM without DOX was similar to wild-type cells, while with DOX induction, the amount of sterol in the cell increased to 220 fg/cell (±15 fg/cell). Ergosterol was evident at near trace levels of 0.1–0.3 fg/cell, as judged by routine GC-MS analysis using the SIM mode selecting for ions at m/z 396, 381, and 363 (Fig. 3E inset). GC-MS analysis showed that the major endogenously formed sterols of *Tb*SMT and *Tb*SDM knockdown parasites were cholesta-8,24-dienol (RRT$_c$ 1.06; M$^+$ at m/z 384), cholesta-7,24-dienol (RRT$_c$ 1.15; M$^+$ at m/z 384), cholesta-5,7,24-trienol (RRT$_c$ 1.10; M$^+$ at m/z 382), lanosterol (RRT$_c$ 1.31; M$^+$ at m/z 426), 31-norlanosterol (RRT$_c$ 1.15; M$^+$ at m/z 412), 14α-methylzymosterol (RRT$_c$ 1.07; M$^+$ at m/z 398), 14α-methyl ergosta-8,25(27)-dienol (RRT$_c$ 1.14; M$^+$ at m/z 412), and 4α,14α-diemethyl ergosta-8,25(27)-dienol (RRT$_c$ 1.24; M$^+$ at m/z 426) (Fig. 3F; supplementary Figs. 4, 5; Table 1).
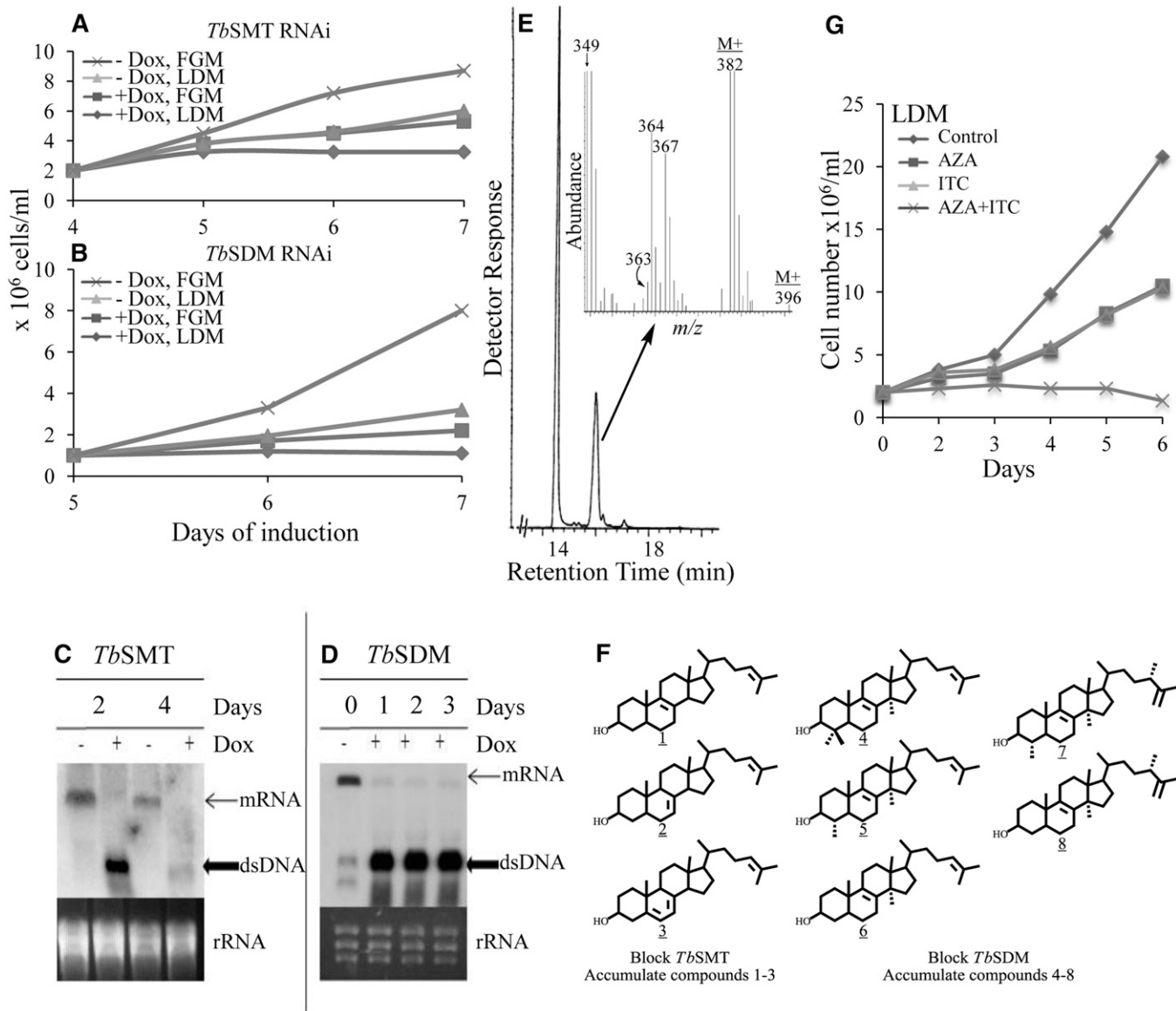
Fig. 3. Effect of RNAi knockdown and inhibitor treatment of *Tb*SMT and *Tb*SDM in PCF. Growth of control engineered cells from the *Tb*SMT RNAi line (A) and the *Tb*SDM RNAi line (B) in FGM and LDM in the absence and presence of DOX. Growth curves were performed in triplicate conducting three independent experiments described in the Experimental Procedures; error bars are not shown because, in most cases, they approximate the data symbols. mRNA steady state levels and dsRNA induction of *Tb*SMT (C) and *Tb*SDM (D) analyzed by Northern blot as described in the Experimental Procedures. Partial total ion current chromatogram of DOX-induced *Tb*SMT cells harvested from 3 to 5 days; inset above GC peak of cholesta-5,7,24-trienol overlapping ergosterol corresponds to the enhanced high end mass spectrum (E). Structures of compounds that accumulate in *Tb*SMT and *Tb*SDM RNAi cells lines and in treated cells, as reported in supplementary Table 1 (F). Growth of PCF in LDM without inhibitor (diamond symbol), or with ED$_{50}$ concentrations of either AZA or ITC (square and triangle symbols, respectively), or a combination of AZA and itraconzaole at ED$_{50}$ concentrations (× symbol) (G).

The accumulation of endogenously formed 14α-methyl sterols, which might be considered as toxic intermediates, was not particularly pronounced in the DOX-induced RNAi lines. DOX-induced *Tb*SMT and *Tb*SDM RNAi lines produced minor amounts of endogenously formed sterol, while cholesterol from the media was the major cellular sterol (Table 1). Together, our results show that the ergosterol biosynthesis pathway remains similar to wild-type cells following reduction of *Tb*SMT or *Tb*SDM by RNAi. Thus an incomplete inhibition of growth in DOX-induced RNAi cell lines, despite the decrease in ergosterol biosynthesis, can be understood, as downregulation or inhibition

of the target enzymes is not quite complete and the reduced ergosterol level is still sufficient to maintain an adequate amount of signal molecule to spark growth.

To further examine the importance of *Tb*SMT and *Tb*-SDM enzymes in PCF growth in a manner complementary to RNAi silencing, we exposed wild-type cells to increasing concentrations of AZA, 25-thialanosterol sulfonium salt, or ITC, drugs which should inhibit these enzymes for mechanistic reasons (supplementary Fig. 6) (4, 44). Cell growth of wild-type PCF in FGM at day 6 was inhibited in a dose-dependent manner of ED$_{50}$ values from 1 to 3 µM; there was no significant difference in the ED$_{50}$ values for

cells cultured in LDM (Fig. 3G). The dose causing a 50% cell growth inhibition at ED_{50} <10 µM being proposed as a threshold to consider a compound as a potential anti-sleeping sickness drug (45). When the PCF cells were exposed to AZA, 25-thialanosterol sulfonium salt, or ITC, the sterol mixture of treated cells was the same as reported previously for the TbSMT and TbSDM RNAi cell lines, but in different proportions depending on the concentration of inhibitor added to the media (Fig. 3G; supplementary Table 1). Cells treated with the inhibitors in FGM grow in a similar manner to treated cells in LDM (supplementary Fig. 7) and accumulate cholesterol proportional to the degree of inhibition imposed on the target enzyme; at the ED_{50} drug concentration, cholesterol represents approximately 50% of the total sterol, while at the ED_{90} drug concentration, cholesterol represents approximately 90% total sterol. The amount of total sterol in these cells ranged from 145 fg/cell at ED_{50} to 160 fg/cell at the ED_{90}, which is similar to control. Ergosterol could not be detected in any of the treated cells in routine GC-MS analyses.

In fully developed cultures at the IC_{99} value, cells can survive for several days, as these cells were shown to contain a full complement of endogenously formed sterols of cholesterol to 24-deasalkyl sterol:24-alkyl sterol [mostly ergosta-5,7,25(27)-trienol] in a ratio of 66:33:1 (AZA) and 40:57:3 (25-thialanosterol sulfonium salt), and to contain significantly more total sterol than controls at approximately 302 fg/cell (±15 fg/cell). These observations show that the inability of potent inhibitors of TbSMT to be toxic to PCF at high drug concentrations could result from a feedback response that signals upregulation of ergosterol biosynthesis enzymes to overcome the effect of the inhibitor. As the response of the cells to inhibitors of TbSMT and TbSDM failed to lead to cell death, the unexpected results just recorded at the ED_{99} drug concentration prompted us to examine the effects of combining two drugs on growth by cells kept in FGM or LDM. When AZA was combined with ITC at approximately the ED_{50} values of 1 µM, minimal growth was observed for cells cultured in FGM, but in LDM a no growth response was observed with cell fragments apparent microscopically showing cell death (Fig. 3G, supplementary Fig. 8). Although cholesterol available from the serum could provide a buffering capacity in membranes to counter the potentially toxic 14α-methyl sterol intermediates (46, 47), cells died in LDM, nonetheless, when the media was supplemented with a combination of the two drugs (Fig. 3G). The foregoing results imply that the reason why PCFs are responsive to ergosterol biosynthesis inhibitors is that small amounts of ergosterol are required for essential cell functions, rather than that they accumulate unusual sterols which may perturb membrane structures.

Kinetic analysis

Kinetic studies were carried out to investigate the interaction of TbSMT and the test drugs. Previously, the TbSMT was cloned and the optimal substrate for activity shown as zymosterol (K_m = 47 µM, k_{cat} = 0.6 min^{-1}) affording a catalytic competence (V_{max}/K_m) of 0.13 (8). The enzyme is known to be a tetramer and catalyze an irreversible reaction with SAM binding first (48). The substrate-based inhibitors examined with TbSMT were reversible transition state analogs in which the protonated or salt form of the molecule mimicked the carbonium ion intermediate in the C24-methylation reaction. Thus, K_i values for AZA and 25-thialanosterol sulfonium salt determined over the concentration range of 25–75 nm with TbSMT were 39 nM (noncompetitive against zymosterol) and 86 nM (noncompetitive against zymosterol), respectively, while the K_i value for lanosterol examined over the concentration range of 15–150 µM was 126 µM (competitive against zymosterol) (supplementary Fig. 9). The K_i/K_m values of 39 nm/47 µM = 0.008 and 86 nM/47µM = 0.018 for AZA and 25-thialanosterol sulfonium salt, respectively, compared with the K_i/K_m value of 126 µM/47 µM = 2.6 for lanosterol indicate that the test compounds are potent transition state analogs of TbSMT catalysis, which interrupt the C24-methylation reaction as shown for the fungal SMT (49–51).

The TbSDM was also cloned and characterized previously (6), and the optimal substrate was shown as 31-norlanosterol (K_m = 9 µM and k_{cat} = 4 min^{-1}) with a catalytic competence of 0.43. Azole drugs have been shown to be tight binding inhibitors of the TbSDM (6). We have not examined ITC against the isolated TbSDM; however, a similar azole (ketoconazole) was found to generate a K_d of approximately 4 µM against the cloned TbSDM (51). The accumulation of specific 24-desalkyl sterol and 14α-methyl sterols coupled to the suppression of growth from the test inhibitors agrees with the substrate specificities of the target enzymes.

Effects of inhibitors and RNAi treatment of TbSMT on BSF growth and in vivo infections

All the test drugs demonstrated a clear dose-dependent inhibitory effect on BSF cells cultured in FGM (supplementary Figs. 8, 11) with ED_{50} values that ranged from 1 to 3 µM, while they failed to inhibit cultured HEK cells at greater than or equal to 50 µM (Table 1) (45). Thus, the relative trypanocidal activity for each compound affording a therapeutic index <25 (ED_{50} against the mammalian cell line/ED_{50} against the parasite) is similar to the action of commercial drugs used to treat first- or second-stage sleeping sickness, such as suramin, ED_{50} of 0.4 µM and nifurtimox and eflornithine combination therapy of 5 µM (52). In view of successes with azoles to treat Chagas disease (53, 54) and our observations with combinations of AZA and ITC to kill PCF cells, we tested the possibility of drug synergism as an approach to inhibit BSF growth. Thus, by combining AZA at ED_{50} with ITC at ED_{50}, BSF growth in LDM led to cell death or to marked growth inhibition in FGM (supplementary Fig. 10).

In a first attempt to test whether there is an ergosterol-dependent disease process linked to *T. brucei* infections, we examined the response of mice infected with BSF cells engineered for RNAi-mediated depletion of TbSMT or infected with wild-type BSF and treated with inhibitors of TbSMT. Preliminary studies showed DOX-induced knockdown of TbSMT in BSF failed to prevent growth, although cells cultured in LDM grew to a lower population density than cells

cultured in FGM (**Fig. 4**, for PCF cultures in FGM see supplementary Fig. 11). Northern blot analysis of total RNA showed that induction of RNAi was effectively complete by day 4 (Fig. 4B). GC-MS analysis of cells harvested between 3 and 5 days showed cholesterol as the major cellular sterol (<99%) in agreement with wild-type controls (4).

Next, we tested mice infected with *T. brucei* strain 427 engineered with DOX-inducible *Tb*SMT RNAi and treated mice with a wild-type strain with AZA or 25-thialanosterol sulfonium salt. To assess the virulence of *Tb*SMT RNAi cells, Balb/C mice (eight per group) were either left untreated (uninduced control) or treated with DOX in their drinking water to induce *Tb*SMT RNAi. Mice were then infected intraperitoneally with 1×10^4 freshly prepared BSF *Tb*SMT RNAi trypanosomes. The uninduced control infection resulted in a mean-time-to-death of 8–9 days. However, when *Tb*SMT RNAi was induced in the DOX-treated mice, there

was protection against death that extended their life for another 4–11 days. Northern blot analysis of BSF isolated from day 13 infected mice clearly indicated the *Tb*SMT gene was transcribed at a level approximately one-sixth that recorded for procyclic cells cultured on FGM (Fig. 4C). In a separate study with mice, the animals were infected with BSF and 5 mg/kg of inhibitor at one dose per day to conserve drug. As with the knockdown *Tb*SMT lines, survival was extended for at least 2 days (Fig. 4D). The survival results from the two experiments complement each other and show that C24-methylation of the ergosterol side chain is functionally important for full virulence in mice.

Small amounts of ergosterol are essential for cell proliferation

To determine whether the absence of ergosterol production is responsible for the growth phenotype observed
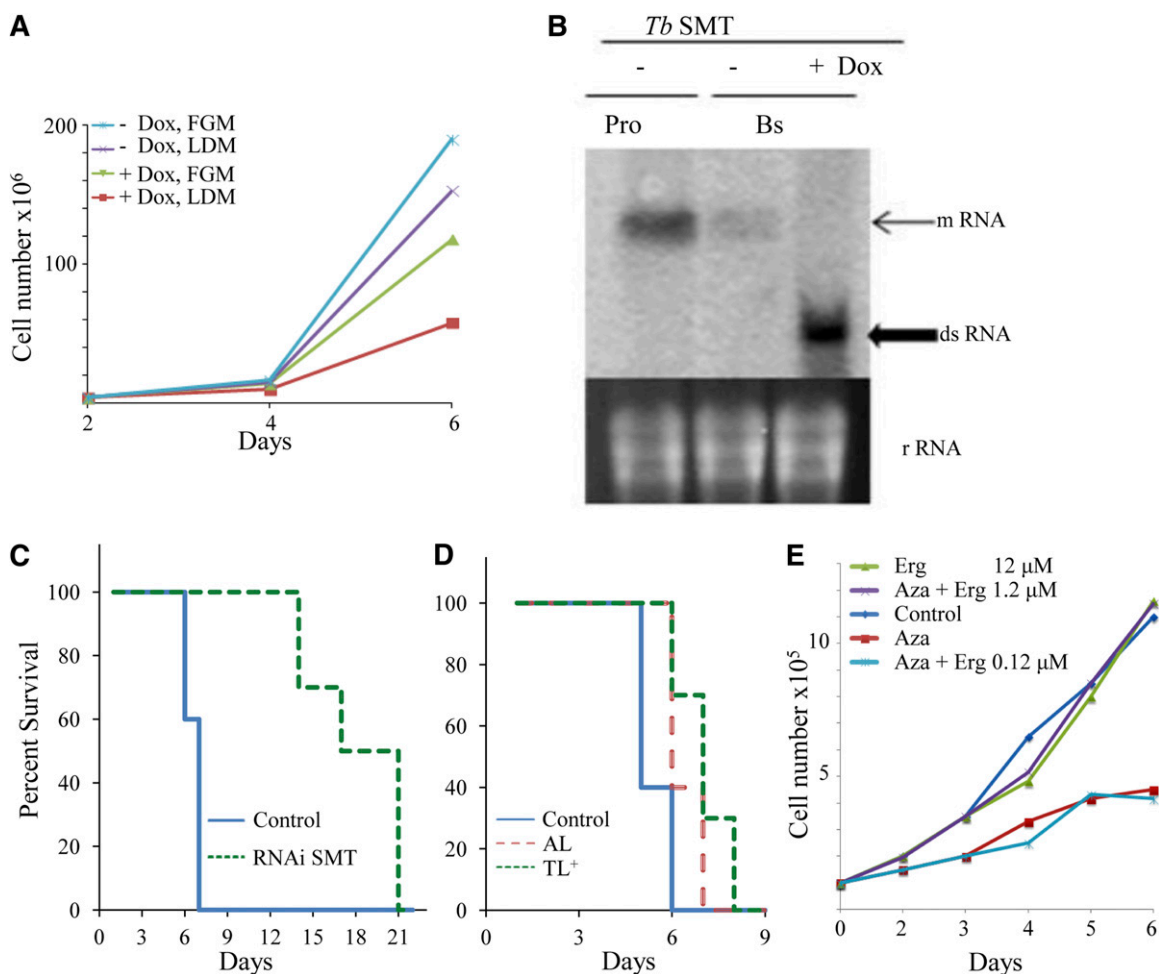

Fig. 4. Growth of BSFs cultured in vitro with and without inhibitor treatment in FGM or LDM and Kaplan-Meier survival analysis of mice infected with and without DOX-induced *Tb*SMT RNAi cells and with inhibitors of *Tb*SMT. A: *Tb*SMT RNAi strain cultured with and without DOX in FGM or LDM. B: Northern blot of *Tb*SMT RNAi cell line. Pro, PCF; Bs, BSF. C: Survival data for *T. brucei*-infected mice. Solid blue line, control group (infected, wild-type BSF); dashed green line (infected, *Tb*SMT RNAi BSF cell line). D: Survival data for *T. brucei*-infected mice. Solid blue line, control group (infected, wild-type BSF); red dashed line, AZA; and green-dotted line, 25-thialanosterol sulfonium salt (TL+), treated mice at 5 mg/kg. E: Rescue experiment of BSF-*Tb*SMT RNAi cells in FGM supplemented with AZA at 1 μM (ED$_{50}$ concentration) with increasing concentrations of ergosterol (Erg) as shown. For all panels, the average of three replicates is shown. Error bars are not shown because, in most cases, they approximate the data symbols.

using ergosterol biosynthesis inhibitors, we developed conditions in which the background of ergosterol could be brought to insignificant levels by culturing the *Tb*SMT RNAi cell line in LDM with AZA, affording continued synthesis of cholesta-5,7,24-trieno,l while growth was restricted to less than 1.5×10^5 cells/ml by day 2 and 4.5×10^5 cells/ml by day 6 (Fig. 4E). Figure 4E shows the growth response of BSF cultured in LDM supplemented with a fixed concentration of AZA at IC_{90}, a synergistic mixture of 7.8 µM cholesterol (3 µg/ml from the serum lipids) and varied concentrations of ergosterol, which ranged from 0.12 µM to 12 µM [at 0 µg/ml, 0.12 µM; 0.05 µg/ml (1:60 ergosterol/cholesterol), 1.2 µM; 0.5 µg/ml (1:7 ergosterol/cholesterol), 12 µM; and 5.0 µg/ml (3/5 ergosterol/cholesterol)]. At 0.12 µM ergosterol, cells did not grow. However, at 1.2 µM ergosterol, giving 1:7 ratio of ergosterol to cholesterol, the growth was completely rescued. Neither the doubling time nor the yield was affected by further supplementation of ergosterol at 12 µM. To determine whether a 14-methyl sterol intermediate could replace ergosterol and spark growth of PCF or BSF, lanosterol was added at increasing concentrations from 0.1 µM to 12 µM to the LDM media supplemented with AZA. In these experiments, lanosterol failed to spark growth, such that the RNAi cell lines continued to show a no growth response after a 6 day incubation period. These results show that ergosterol with a 24β-methyl group is necessary for cell viability and proliferation in small amounts, so long as another Δ^5-sterol with a 24-H atom, such as cholesterol, is present in large amounts.

DISCUSSION

The sensitivity of trypanosomatid protozoa to regulation of ergosterol biosynthesis by gene silencing and inhibitors offers a unique opportunity for understanding ergosterol biology, drug target identification, and the subsequent development of new anti-parasite agents. In the present work, we explored the little understood multiple functions of sterols in parasite growth by analyzing the sterol composition of PCF and BSF cells and correlating this information to growth responses resulting from the knockdown of *Tb*SMT and *Tb*SDM gene expression and blocking *Tb*SMT and *Tb*SDM action involved with ergosterol biosynthesis. This approach showed that PCF and BSF can live with variable, albeit minute, amounts of ergosterol, as long as prevalent cholesterol is available from the host to serve as the architectural component of membranes. We were able to pinpoint the vastly different natural concentrations of ergosterol associated with growth of PCF and BSF cultured in FGM as 6 fg/cell or 0.01 fg/cell, respectively. In contrast, the overall sterol composition of these cells remain fairly constant at 150 fg/cell, and cholesterol can contribute from 50 to <99% of the total sterol, depending on culture conditions. Notably, alterations in cholesterol environment by changing the FGM to LDM media, which mirrors cholesterol availability in human blood and insects, respectively (24, 55), can decrease ergosterol biosynthesis in cells and suppress growth rates of PCF or BSF. The most logical explanation for this association involves a stage-specific relationship between the biosynthetic renewal of ergosterol and cell proliferation.

Ergosterol, at near hormonal levels in cells, has been implicated as a signal molecule of variant nonpathogenic microorganisms (26). By virtue of the RNAi silencing and inhibitors designed specifically to prevent *Tb*SMT and *Tb*-SDM catalysis, it has been possible to block complete metabolism of lanosterol to ergosterol, which results in high cholesterol import, while there is only minor accumulation of intermediates under normal metabolic conditions. In contrast, Perez-Moreno et al. (56) failed to observe any antiproliferative effects of 22,26-azasterol on the procyclic parental line of *T. brucei* or of induced (+DOX) or noninduced (−DOX) after 6 days of *Tb*SMT interference or detected any ergosterol in these cells. Our results demonstrate that the virtually complete replacement of endogenously formed sterols by cholesterol is not compatible with cell growth unless small amounts of ergosterol are available to spark cell proliferation. In the present experiments, the quantities of sterol supplied to the media found necessary to rescue PCF or BSF cultures that were devoid of ergosterol were similar to other microorganisms auxotrophic for sterol. Additionally, the minimal synergistic mixture of ergosterol and cholesterol in a 1:7 ratio used to promote growth is similar to the combination of ergosterol and cholesterol provided to GL7 yeast to spark its growth (26). The results show a commonality in ergosterol function across kingdoms distinct from the bulk membrane role. The failure of earlier workers to find ergosterol in BSF (55) probably has its origins in the experimental difficulties in the methods one uses in recognizing ergosterol from its isomers or detecting ergosterol as a trace component eluting underneath cholesta-5,7,24-trienol in GC-MS analysis.

In the case of parasitic diseases, there are very few validated enzyme targets. The only drug for which there is a well-defined molecular target is eflornithine, an analog of ornithine which blocks spermidine synthesis and the formation of trypanothione through irreversible inhibition of ornithine decarboxylase; administered with nifurtimox, the combination therapy has enjoyed rapid implementation (52). Based on previous successes with substrate analogs containing nitrogen or sulfur on the lateral sterol side chain proving them to be potent antifungal agents (5, 49–51), we studied two of them, AZA and 25-thialanosterol sulfonium salt, as reversible tight-binding inhibitors of *Tb*-SMT. When these compounds were examined for effects on cell growth, ergosterol biosynthesis, and inhibition of the cloned *Tb*SMT, it became evident that *Tb*SMT is crucial for life support and is assayable and druggable, and that these trypanocidal agents may exhibit a limited drug resistance when used synergistically with another mechanism-based inhibitor which can block at a different step in the late-stages of ergosterol biosynthesis. It is interesting that as the concentration of the AZA is increased to ED_{99}, rather than forcing an accumulation of harmful intermediates that cause cells to die, they continued to live due to

a compensatory upregulation in ergosterol biosynthesis. However, when AZA was combined with itraconzaole at their ED$_{50}$, cell proliferation stopped and cells died. The total dependence of inhibitor-treated cells on ergosterol for sparking cell proliferation is thus understandable and can be reconciled with all experimental observations, by their depletion of ergosterol production, and may turn out to be useful in the design of a new generation of ir-reversible suicide substrates targeted to impair essential sterol functions in trypanosomes (8, 57). All things considered, due to the limits of monotherapies, greater emphasis should be placed on orally administered analogs of *Tb*SMT catalysis in combination with specific azoles, which together might be effective in smaller amounts and have less deleterious effects on the host than the drugs presently in use.▪

REFERENCES

1. Simarro, P. P., J. Jannin, and P. Cattand. 2008. Eliminating human African trypanosomiasis: where do we stand and what comes next? *PLoS Med.* **5:** e55.
2. World Health Organization. 2012. Trypanosomiasis, human African (sleeping sickness). Accessed July 14, 2013, at http://www.who.int/mediacentre/factsheets/fs259/en/.
3. Simarro, P. P., J. R. Franco, G. Cecchi, M. Paone, A. Diarra, J. A. Ruiz Postigo, and J. G. Jannin. 2012. Human African trypanosomiasis in non-endemic countries (2000–2010). *J. Travel Med.* **19:** 44–53.
4. Zhou, W., G. A. M. Cross, and W. D. Nes. 2007. Cholesterol import fails to prevent catalyst inhibition of ergosterol synthesis and cell proliferation of *Trypanosoma brucei*. *J. Lipid Res.* **48:** 665–675.
5. Nes, W. D., W. Zhou, K. Ganapathy, J. Liu, R. Vatsyayan, S. Chamala, K. Hernandez, and M. Miranda. 2009. Sterol C24-methyltransferase: an enzymatic target for the disruption of ergosterol biosynthesis and homeostasis in *Cryptoccoccus neoformans*. *Arch. Biochem. Biophys.* **481:** 210–218.
6. Nes, C. R., U. K. Singha, J. Liu, K. Ganapathy, F. Villalta, M. R. Waterman, G. I. Lepesheva, M. Chaudhuri, and W. D. Nes. 2012. Novel metabolic network of *Trypanosoma brucei* procyclic and bloodstream forms. *Biochem. J.* **443:** 267–277.
7. Miller, M. B., B. A. Haubrich, Q. Wang, W. J. Snell, and W. D. Nes. 2012. Evoutionary conserved $\Delta^{25(27)}$-olefin ergosterol biosynthesis pathway in the alga *Chlamydomonas reinhardtii*. *J. Lipid Res.* **53:** 1636–1645.
8. Zhou, W., G. I. Lepesheva, M. R. Waterman, and W. D. Nes. 2006. Mechanistic analysis of a multiple product sterol methyltransferase implicated in ergosterol biosynthesis in *Trypanosoma brucei*. *J. Biol. Chem.* **281:** 6290–6296.
9. Dixon, H., C. D. Ginger, and J. Williamson. 1972. Trypanosome sterols and their metabolic origins. *Comp. Biochem. Physiol. B.* **41:** 1–18.
10. Coppens, I., T. Levade, and P. J. Courtoy. 1995. Host plasma low density lipoprotein particles as an essential source of lipids for the bloodstream forms of *Trypanosoma brucei*. *J. Biol. Chem.* **270:** 5736–5741.
11. Coppens, I., and P. J. Courtoy. 1995. Exogenous and endogenous sources of sterols in the culture-adapted procyclic trypomastigotes of *Trypanosoma brucei*. *Mol. Biochem. Parasitol.* **73:** 179–188.
12. Green, H. P., M. P. Molina Portela, E. N. St. Jean, E. B. Lugli, and J. Raper. 2003. Evidence for a *Trypanosoma brucei* lipoprotein scavenger receptor. *J. Biol. Chem.* **278:** 422–427.
13. Löw, P., G. Dallner, S. Mayor, S. Cohen, B. T. Chait, and A. K. Menon. 1991. The mevalonate pathway in the bloodstream form of *Trypanosoma brucei*. *J. Biol. Chem.* **266:** 19250–19257.
14. Matsumori, N., K. Tahara, H. Yamamoto, A. Morooka, M. Doi, T. Oishi, and M. Murata. 2009. Direct interaction between amphotericin B and ergosterol in lipid bilayers as revealed by ^{2}H NMR spectroscopy. *J. Am. Chem. Soc.* **131:** 11855–11860.
15. Thornton, S. J., and K. M. Wasan. 2009. The reformulation of amphotericin B for oral administration to treat systemic fungal infections and visceral leishmaniasis. *Expert Opin. Drug Deliv.* **6:** 271–284.
16. Fügi, M. A., K. Gunasekera, T. Ochsenreiter, X. Guan, M. R. Wenk, and P. Maser. 2014. Genome profiling of sterol synthesis shows convergent evolution in parasites and guides chemotherapeutic attack. *J. Lipid Res.* **55:** 929–938.
17. Queiroz, R., C. Benz, K. Fellenberg, J. D. Hoheisel, and C. Clayton. 2009. Transcriptome analysis of differentiating trypanosomes reveals the existence of multiple post-transcriptional regulons. *BMC Genomics.* **10:** 495–515.
18. Lepesheva, G. I., R. D. Ott, T. Y. Hargrove, Y. Y. Kleshchenko, I. Schuster, W. D. Nes, G. C. Hill, F. Villalta, and M. R. Waterman. 2007. Sterol 14α-demethylase as a potential target for antitrypansomal therapy: Enzyme inhibition and parasite growth. *Chem. Biol.* **14:** 1283–1293.
19. Gros, L., S. O. Lorente, C. Jimenez, V. Yardley, L. Rattray, H. Wharton, S. Little, S. L. Croft, L. M. Ruiz-Perez, D. Gonzalez-Pacanowska, et al. 2006. Evaluation of azasterols as anti-parasitics. *J. Med. Chem.* **49:** 6094–6103.
20. Gigante, F., M. Kaiser, R. Brun, and I. H. Gilbert. 2009. SAR studies on azasterols as potential anti-trypanosomal and anti-leshmania agents. *Bioorg. Med. Chem.* **17:** 5950–5961.
21. Bloch, K. 1991. Cholesterol: evolution of structure and function. *In* Biochemistry of Lipids, Lipoproteins and Membranes. D. E. Vance and J. Vance, editors. Elsevier, New York. 363–381.
22. Hartman, M-A. 1998. Plant sterols and the membrane environment. *Trends Plant Sci.* **3:** 170–175.
23. Hildenbrand, M. F., and T. M. Bayerl. 2005. Differences in the modulation of collective membranes motions by ergosterol, lanosterol, and cholesterol: a dynamic light scattering study. *Biophys. J.* **88:** 3360–3367.
24. Nes, W. D. 2011. Biosynthesis of cholesterol and other sterols. *Chem. Rev.* **111:** 6423–6451.
25. Rodriguez, R. J., and L. W. Parks. 1983. Structural and physiological features of sterols necessary to satisfy bulk and sparking requirements in yeast sterol auxotrophs. *Arch. Biochem. Biophys.* **225:** 861–871.
26. Ramgopal, M., and K. Bloch. 1983. Sterol synergism is yeast. *Proc. Natl. Acad. Sci. USA.* **80:** 712–715.
27. Xu, F., S. D. Rychonovsky, J. D. Belani, H. H. Hobbs, J. C. Cohen, and R. B. Rawson. 2005. Dual role for cholesterol in mammalian cells. *Proc. Natl. Acad. Sci. USA.* **102:** 14551–14556.
28. Bittman, R. 1997. Has nature designed the cholesterol side chain for optimal interaction with phospholipids? *Subcell. Biochem.* **28:** 145–171.
29. Rodriguez, R. J., C. Low, C. D. Bottema, and L. W. Parks. 1985. Multiple functions for sterols in *Saccharomyces cerevisiae*. *Biochim. Biophys. Acta.* **837:** 336–343.
30. Aguilar, P. S., M. G. Heiman, T. C. Walther, A. Engel, D. Schwudke, N. Gushwa, T. Kurzchalia, and P. Walter. 2010. Structure of sterol aliphatic chains affects yeast cell shape and cell fusion during mating. *Proc. Natl. Acad. Sci. USA.* **107:** 4170–4175.
31. Pinto, W. J., and W. R. Nes. 1983. Stereochemical specificity for sterols in *Saccharomyces cerevisiae*. *J. Biol. Chem.* **258:** 4472–4476.
32. Gilbert, I. H. 2013. Drug discovery for neglected diseases: molecular target-based and phenotypic approaches. *J. Med. Chem.* **56:** 7719–7726.
33. Ferrins, L., R. S. Rahmani, and J. B. Baell. 2013. Drug discovery and human African trypanosomiasis: a disease less neglected? *Future Med. Chem.* **5:** 1801–1841.
34. Kanagasabai, R., W. Zhou, J. Liu, T. T. Minh Nguyen, P. Veeramachaneni, and W. D. Nes. 2004. Disruption of ergosterol biosynthesis, growth and the morphological transition in *Candida albicans* by sterol methyltransferase inhibitors containing sulfur at C-25 in the sterol side chain. *Lipids.* **39:** 737–746.
35. Nes, W. D., D. Guo, and W. Zhou. 1997. Substrate-based inhibitors of the (S)-adenosyl-L-methionine:delta24(25)- to delta24(28)-sterol methyltransferase from *Saccharomyces cerevisiae*. *Arch. Biochem. Biophys.* **342:** 68–81.
36. Singha, U. K., V. Hamilton, M. R. Duncan, E. Weems, M. K. Tripathi, and M. Chaudhuri. 2012. Protein translocase of mitochondrial inner membrane in *Trypanosoma brucei*. *J. Biol. Chem.* **287:** 14480–14493.
37. Biebinger, S., L. E. Wirtz, P. Lorenz, and C. Clayton. 1997. Vectors for inducible expression of toxic gene products in bloodstream and procyclic *Trypanosoma brucei*. *Mol. Biochem. Parasitol.* **85:** 99–112.

38. Pan, C., X. Bai, Y. Ji, X. Li, and Q. Chen. 2005. Cytoprotection by glycine against ATP-induced injury is mediated by glycine receptor in renal cells. *Biochem. J.* **390:** 447–453.
39. Kim, S. Y., W. Hur, J. E. Choi, D. Kim, J. S. Wang, H. Y. Yoon, L. S. Piao, and S. K. Yoon. 2009. Functional characterization of human oncoprotein gankyrin in Zebrafish. *Exp. Mol. Med.* **41:** 8–16.
40. Vanhollebeke, B., and E. Pays. 2010. The trypanolytic factor of human serum: many ways to enter the parasite, a single way to kill. *Mol. Microbiol.* **76:** 806–814.
41. Sharma, S., U. K. Singha, and M. Chaudhuri. 2010. Role of Tob55 on mitochondrial protein biogenesis in *Trypanosoma brucei*. *Mol. Biochem. Parasitol.* **174:** 89–100.
42. Nes, W. D., P. Jayasimha, and Z. Song. 2008. Yeast sterol C24-methyltransferase: role of highly conserved tyrosine-81 in catalytic competence studied by site-directed mutagenesis and thermodynamic analysis. *Arch. Biochem. Biophys.* **477:** 313–323.
43. Wickstead, B., K. Ersfeld, and K. Gull. 2002. Targeting of a tetra-cycline-inducible expression system to the transcriptionally silent minichromosomes of *Trypanosoma brucei*. *Mol. Biochem. Parasitol.* **125:** 211–216.
44. Lepesheva, G. I., H. Park, T. Y. Hargrove, B. Vanhollebeke, Z. Wawrzak, J. M. Harp, M. Sundaramoorthy, W. D. Nes, E. Pays, M. Chaudhuri, et al. 2010. Crystal structures of *Trypanosoma brucei* sterol 14α-demethylase and implications for selective treatment for human infections. *J. Biol. Chem.* **285:** 1773–1780.
45. Hoet, S., F. Opperdoes, R. Brun, and J. Quetin-Leclercq. 2004. Natural products active against African trypanosomes: a step towards new drugs. *Nat. Prod. Rep.* **21:** 353–364.
46. Vanden Bossche, H., P. Marichal, M. C. Coene, G. Willemsens, L. Le Jeune, W. Cools, and H. Verhoeven. 1992. Cytochrome P450—dependent 14α-demethylase: target for antifungal agents and herbicides. *Amer. Chem. Soc. Ser.* **497:** 219–230.
47. Kelly, S. L., D. C. Lamb, A. J. Corran, B. C. Baldwin, and D. E. Kelly. 1995. Mode of action and resistance to azole antifungals associated with the formation of 14α-methylergosta-8,24-dienol-3β, 6α-hydroxy-diol. *Biochem. Biophys. Res. Commun.* **207:** 910–915.
48. Nes, W. D., Z. Song, A. L. Dennis, W. Zhou, J. Nam, and M. B. Miller. 2003. Biosynthesis of phytosterols: Kinetic mechanism for the enzymatic C-methylation of sterols. *J. Biol. Chem.* **278:** 34505–34516.
49. Ganapathy, K., R. Kanagasabai, T. T. M. Nguyen, and W. D. Nes. 2011. Purification characterization and inhibition of sterol C24-methyltransferase from *Candia albicans*. *Arch. Biochem. Biophys.* **505:** 194–201.
50. Oehlschlager, A. C., R. H. Angus, A. M. Pierce, H. D. Pierce, and R. Srinivasan. 1984. Azasterol inhibition of Δ24-sterol methyltransferase in *Saccharomyces cerevisiae*. *Biochemistry*. **23:** 3582–3589.
51. Lepesheva, G. I., W. D. Nes, W. Zhou, G. C. Hill, and M. R. Waterman. 2004. CYP51 from *Trypanosoma brucei* is obtusifoliol-specific. *Biochemistry*. **43:** 10789–10799.
52. Vincent, I. M., D. Creek, D. G. Watson, M. A. Kamleh, D. J. Woods, P. E. Wong, R. J. S. Burchmore, and M. P. Barrett. 2010. A molecular mechanism for eflornithine resistance in African trypanosomes. *PLoS Pathog.* **6:** e1001204.
53. Maldonado, R. A., J. Molina, G. Payares, and J. A. Urbina. 1993. Experimental chemotherapy with combinations of ergosterol biosynthesis inhibitors in murine models of Chagas' disease. *Antimicrob. Agents Chemother.* **37:** 1353–1359.
54. Villalta, F., M. C. Dobish, P. N. Nde, Y. Y. Kleshchenko, T. Y. Hargrove, C. A. Johnson, M. R. Waterman, J. N. Johnson, and G. I. Lepesheva. 2013. VNI cures the acute and chronic experimental Chagas disease. *J. Infect. Dis.* **208:** 504–511.
55. Behmer, S. T., and W. D. Nes. 2003. Insect sterol nutrition and physiology: a global overview. *Adv. In Insect Phys.* **31:** 1–72.
56. Pérez-Moreno, G., M. Sealey-Cardona, C. Rodrigues-Poveda, M. H. Gelb, L. M. Ruiz-Perez, V. Castillo-Acosta, J. A. Urbina, and D. Gonzalez-Pacanowska. 2012. Endogenous sterol biosynthesis is important for mitochondrial function and cell morphology in procyclic forms of *Trypanosoma brucei*. *Int. J. Parasitol.* **42:** 975–989.
57. Hargrove, T. Y., Z. Wawrzak, J. Liu, M. R. Waterman, W. D. Nes, and G. I. Lepesheva. 2012. Structural complex of sterol 14α-demethylase (CYP51) with 14α-methylenecyclopropyl-Δ7-24,25-dihydrolanosterol. *J. Lipid Res.* **53:** 311–320.